Weierstraß-Institut
für Angewandte Analysis und Stochastik

im Forschungsverbund Berlin e.V.

Preprint ISSN 0946 – 8633

Slow motion of quasi-stationary multi-pulse solutions by semistrong interaction in reaction-diffusion systems

Matthias Wolfrum[1] , Julia Ehrt[1]

submitted: 11th June 2007

[1] Weierstrass Institute for Applied Analysis and Stochastics
Mohrenstraße 39
D – 10117 Berlin
Germany
E-Mail: wolfrum@wias-berlin.de
E-Mail: ehrt@wias-berlin.de

No. 1233
Berlin 2007

2000 *Mathematics Subject Classification.* 35B25, 34C30, 35K57.

Key words and phrases. pulse interaction, singular perturbation theory.

Edited by
Weierstraß-Institut für Angewandte Analysis und Stochastik (WIAS)
Mohrenstraße 39
10117 Berlin
Germany

Fax: + 49 30 2044975
E-Mail: preprint@wias-berlin.de
World Wide Web: http://www.wias-berlin.de/

Abstract

In this paper, we study a class of singularly perturbed reaction-diffusion systems, which exhibit under certain conditions slowly varying multi-pulse solutions. This class contains among others the Gray-Scott and several versions of the Gierer-Meinhardt model. We first use a classical singular perturbation approach for the stationary problem and determine in this way a manifold of quasi-stationary N-pulse solutions. Then, in the context of the time-dependent problem, we derive an equation for the leading order approximation of the slow motion along this manifold. We apply this technique to study 1-pulse and 2-pulse solutions for classical and modified Gierer-Meinhardt system. In particular, we are able to treat different types of boundary conditions, calculate folds of the slow manifold, leading to slow-fast motion, and to identify symmetry breaking singularities in the manifold of 2-pulse solutions.

1 Introduction

Reaction diffusion systems show already in one space dimension a large variety of interesting spatio-temporal dynamics. Particularly, pulse solutions play an important role in many biochemical and biological systems [13, 10]. Whereas the existence, stability, and motion of a single pulse is in many cases well understood, the situation of several interacting pulses is much more difficult to analyze. The basic idea to study pulse interaction is the following: As soon as the distance between the pulses is sufficiently large compared to the pulse width, one can describe each pulse locally by a single-pulse solution and then study their interaction in a perturbative way. In cases where the system between the pulses is close to a homogeneous stable stationary state, the pulses interact only via their exponentially decaying tails and hence the pulse motion is exponentially slow with respect to the pulse distance. This phenomenon is usually called *weak interaction*, see [15, 18].

In contrast to that, Doelman and Kaper introduced the notion of *semistrong interaction* (see [3] and references there) for interacting pulses where the background between the pulses is non-homogeneous and far from equilibrium. Like many pattern formation phenomena, semistrong interaction requires the existence of variables with different diffusion lengths. This may lead to solutions, where in between the pulses the system is not close to equilibrium, but shows spatial fluctuations which are governed by the long-ranging diffusion. At the same time, the pulses can be short, because they are governed by another variable with short diffusion length.

As a general model for semistrong pulse interaction, covering several specific models, such as classical and modified Gierer-Meinhardt, Gray-Scott, and others, Doelman and Kaper suggested in [3] the following class of systems:

$$\begin{aligned} \epsilon^2 U_t &= U_{xx} - \epsilon^2 \mu U + f(U)V^2 \\ V_t &= \epsilon^2 V_{xx} - V + g(U)V^2 \end{aligned}$$

We consider positive solutions U and V, for which the functions f and g, as well as the parameters μ and ϵ should be positive. As usual, ϵ is assumed to be small. The spatial variable x is from the interval I, which may be bounded or unbounded. Different types of boundary conditions will be specified later. For convenience, we rescale x here by ϵ and obtain after replacing ϵ^2 by ε the system

$$\begin{aligned} U_t &= U_{xx} - \mu U + \tfrac{1}{\varepsilon} f(U)V^2 \\ V_t &= \varepsilon^2 V_{xx} - V + g(U)V^2. \end{aligned} \tag{1}$$

In this way, ε reflects the ratio of the different diffusion lengths. In the scale of the short diffusion length $\xi = x/\varepsilon$, the system for $u(\xi, t) = U(\varepsilon\xi, t)$, $v(\xi, t) = V(\varepsilon\xi, t)$ is

$$\begin{aligned} u_t &= \tfrac{1}{\varepsilon^2} u_{\xi\xi} - \mu u + \tfrac{1}{\varepsilon} f(u)v^2 \\ v_t &= v_{\xi\xi} - v + g(u)v^2. \end{aligned} \tag{2}$$

Based on the two differently scaled versions (1) and (2), our approach will be somewhat different from that in [3]. In analogy to classical Fenichel theory for singular perturbed systems of ordinary differential equations, we describe in section 2 the set of interacting pulse solutions as a manifold, where the motion vanishes in leading order. In section 3, the slow motion along the manifold is obtained from the next order terms at these quasi-stationary solutions. Finally, in section 4 the general results are used to study manifolds of pulses for the specific nonlinearities from the classical and the modified Gierer-Meinhardt system. In this way, we can explicitely calculate the manifolds of interacting pulse solutions for these systems. In particular, we identify points of normal non-hyperbolicity leading to different scenarios of changes in the stability along the branches of the manifolds. We also demonstrate the existence of non-symmetric two-pulse solutions, which, however, turn out to be not stable. The question of stability or normal hyperbolicity of the obtained manifolds is not addressed analytically in this paper. Instead, we use numerical simulation to give evidence for the dynamical stability at certain parts of the analytically obtained slow-motion manifolds, and to verify the validity of our asymptotic approximation of the slow motion. An analytical study of the spectral problem, which could supply a rigorous proof for normal hyperbolicity and the persistence of the slow manifolds is beyond the scope of the present paper and will be the subject of future investigations.

2 Construction of quasi-stationary N-pulse solutions

The stationary problem for is a singularly perturbed system of ordinary differential equations and, choosing the fine spatial scale from (2), it can be written in the

following form:

$$\begin{aligned} u_\xi &= \varepsilon p && (3)\\ p_\xi &= \varepsilon\mu u - f(u)v^2 && (4)\\ v_\xi &= q && (5)\\ q_\xi &= v - g(u)v^2. && (6) \end{aligned}$$

It is well known for such systems that solutions may consist of fast and slow parts. In this section, we will first solve all these slow and fast parts separately and then derive consistency conditions, which allow us to glue them to leading-order solutions, which are quasi-stationary N-pulse solutions. These quasi-stationary solutions will give rise to a slow-motion manifold for the original PDE. Hence they will not solve the stationary problem in second approximation, and it is not an issue, whether there are true solutions to the stationary problem near these approximating quasi-stationary solutions.

We apply now the standard procedure of singular perturbation theory. We distinguish the fast alias small scale subsystem

$$\begin{aligned} u_\xi &= 0 && (7)\\ p_\xi &= -f(u)v^2 && (8)\\ v_\xi &= q && (9)\\ q_\xi &= v - g(u)v^2, && (10) \end{aligned}$$

obtained by putting $\varepsilon = 0$ in equations (3)–(6), and the slow alias large scale subsystem

$$\begin{aligned} U_x &= P && (11)\\ P_x &= \mu U && (12)\\ 0 &= Q && (13)\\ 0 &= V, && (14) \end{aligned}$$

obtained by rescaling back to x and putting then $\varepsilon = 0$. Note that in principle (14) should be

$$0 = V - g(U)V^2.$$

We are here only interested in the branch corresponding to $V = 0$, which allows to cancel the term $\frac{1}{\varepsilon}f(U)V^2$ in (12), being $O(\varepsilon)$ after substituting $V = O(\varepsilon)$.

The fast subsystem (7)–(10) can be solved explicitely by

$$\begin{aligned} u(\xi) &\equiv a && (15)\\ p(\xi) &= b + \frac{3f(a)}{2g^2(a)}\tanh\left(\frac{\xi}{2}\right)\left(\tanh^2\left(\frac{\xi}{2}\right) - 3\right) && (16)\\ v(\xi) &= \frac{3}{2g(a)}\left(1 - \tanh^2\left(\frac{\xi}{2}\right)\right) && (17)\\ q(\xi) &= -\frac{3}{2g(a)}\tanh\left(\frac{\xi}{2}\right)\left(1 - \tanh^2\left(\frac{\xi}{2}\right)\right). && (18) \end{aligned}$$

These solutions perform a single pulse in v and depend parametrically on a and b. Note that these solutions satisfy $q(0) = 0$, i.e. we have chosen from the family of spatial translates those pulses which are centered at zero. Their behavior at infinity is given by

$$\lim_{\xi\to\pm\infty}(v(\xi)) = \lim_{\xi\to\pm\infty}(q(\xi)) = 0 \tag{19}$$

and

$$\lim_{\xi\to\pm\infty}(p(\xi)) = b \mp \frac{3f(a)}{g^2(a)}, \tag{20}$$

which implies in particular that the pulse in v is accompanied by a step-like profile in p with step-size $\frac{6f(a)}{g^2(a)}$ independent of b (see also equation 2.16 in [3]).

A general solution of the slow system (11)–(14) is given by

$$\begin{aligned} U(x) &= c\cosh(\sqrt{\mu}x) + d\sinh(\sqrt{\mu}x) && (21)\\ P(x) &= \sqrt{\mu}\,(c\sinh(\sqrt{\mu}x) + d\cosh(\sqrt{\mu}x)) && (22)\\ V(x) &\equiv 0 && (23)\\ Q(x) &\equiv 0 && (24) \end{aligned}$$

depending on the two parameters c and d.

We compose now a quasistationary N-pulse by gluing together solutions from the fast and slow subsystem. First, we choose pulse positions $r_1, \ldots, r_N \in I$ in the large spatial scale. In the vicinity of r_j, the quasistationary N-pulse will be given by $u_j(\xi_j; a_j, b_j)$, $p_j(\xi_j; a_j, b_j)$, $v_j(\xi_j; a_j, b_j)$, $q_j(\xi_j; a_j, b_j)$, being a solution (15)–(18) with fixed parameters $a = a_j$ and $b = b_j$, and the space variable

$$\xi_j := \frac{x - r_j}{\varepsilon}. \tag{25}$$

In the intervals between the pulse positions

$$I_j := [r_j, r_{j+1}]$$

we use solutions $U_j(x_j; c_j, d_j)$, $P_j(x_j; c_j, d_j)$, $V_j(x_j; c_j, d_j)$, $Q_j(x_j; c_j, d_j)$ given by (21)–(24) for fixed $c = c_j, d = d_j$, and the space variable

$$x_j := x - r_j. \tag{26}$$

For convenience, we denote the left and right boundary of the whole domain I by r_0 and r_{N+1}, respectively. In this way we get also the two intervals I_0 at the left and I_N at the right boundary, which can be treated in same manner as the others. In the case of periodic boundary conditions, the intervals I_0 and I_N coincide modulo L by choosing $r_0 := r_N - L$ and $r_{N+1} := r_1 + L$, where L is the length of the whole domain I.

At each pulse position r_j, $j = 1 \dots N$, we have to regard the following consistency conditions to assure continuity of the composed solutions in the limit $\varepsilon \to 0$:

$$\begin{aligned} U_{j-1}(y_{j-1}; c_{j-1}, d_{j-1}) &= \lim_{\xi_j \to -\infty} (u_j(\xi_j; a_j, b_j)) && (27) \\ P_{j-1}(y_{j-1}; c_{j-1}, d_{j-1}) &= \lim_{\xi_j \to -\infty} (p_j(\xi_j; a_j, b_j)) && (28) \\ U_j(0; c_j, d_j) &= \lim_{\xi_j \to \infty} (u_j(\xi_j; a_j, b_j)) && (29) \\ P_j(0; c_j, d_j) &= \lim_{\xi_j \to \infty} (p_j(\xi_j; a_j, b_j)). && (30) \end{aligned}$$

Here, we have used the abbreviation $y_j := r_{j+1} - r_j$ for the length of the interval I_j. Note that corresponding consistency conditions for V and v, as well as for Q and q hold true automatically, since they are all necessarily zero at the junctions, see (19) and (23), (24). Inserting now the expressions for the large scale solution according to (21), (22), and the limits of the small scale solution according to (15) and (20), the consistency conditions read as

$$\begin{aligned} c_{j-1} \cosh(\sqrt{\mu} y_{j-1}) + d_{j-1} \sinh(\sqrt{\mu} y_{j-1}) &= a_j && (31) \\ \sqrt{\mu} \left(c_{j-1} \sinh(\sqrt{\mu} y_{j-1}) + d_{j-1} \cosh(\sqrt{\mu} y_{j-1}) \right) &= b_j + \frac{3 f(a_j)}{g^2(a_j)} && (32) \\ c_j &= a_j && (33) \\ \sqrt{\mu} d_j &= b_j - \frac{3 f(a_j)}{g^2(a_j)} && (34) \end{aligned}$$

for $j = 1, ..., N$.

The composed quasistationary N-pulse has to satisfy also the boundary conditions, which will imply additional conditions for the solution parameters. In the case of periodic boundary conditions, we can identify the intervals I_0 and I_N modulo the length L of the domain I and get the additional equations $c_0 = c_N$ and $d_0 = d_N$. In the case of Neumann boundary conditions

$$P_0(0; c_0, d_0) = P_N(y_N; c_N, d_N) = 0$$

we obtain

$$d_0 = \sqrt{\mu} \left(c_N \sinh(\sqrt{\mu} y_N) + d_N \cosh(\sqrt{\mu} y_N) \right) = 0. \quad (35)$$

Analogously, Dirichlet conditions

$$U_0(0; c_0, d_0) = U_N(y_N; c_N, d_N) = 0$$

lead to

$$c_0 = c_N \cosh(\sqrt{\mu} y_N) + d_N \sinh(\sqrt{\mu} y_N) = 0. \quad (36)$$

Note that also inhomogeneous or mixed-type boundary conditions can be treated easily. In the case of an unbounded domain, i.e. $r_0 = -\infty$, we cannot use (26) for

$j = 0$ and define $x_0 := x_1$, instead. Consequently, for $j = 0$ equations (31) and (32) have to be changed to

$$c_0 = a_1 \tag{37}$$

$$\sqrt{\mu} d_0 = b_1 + \frac{3f(a_1)}{g^2(a_1)}. \tag{38}$$

The boundedness condition

$$\lim_{x_0 \to -\infty} (U_0(x_0; c_0, d_0)) = \lim_{x_N \to \infty} (U_N(x_N; c_N, d_N)) = 0$$

leads to the additional equations

$$c_0 = d_0, \qquad c_N = -d_N. \tag{39}$$

In all these cases, we obtain two extra parameter constraints from the boundary conditions. This means that in the $5N + 2$-dimensional space of piecewise solutions, given by the pulse parameters $(a_j, b_j, r_j)_{j=1\ldots N}$ and the background parameters $(c_j, d_j)_{j=0\ldots N}$, there are $4N + 2$ consistency conditions. Thus we can expect that apart from degeneracies there is a N-dimensional manifold $\mathcal{M}_N \subset \mathbf{R}^{5N+2}$ of consistent solution parameters, corresponding for fixed $0 < \varepsilon \ll 1$ to a manifold $\mathcal{M}_N^\varepsilon \subset X$ of quasistationary N-pulse solutions.

3 Slow motion on the manifold of N-pulse solutions

The position of the pulse in the small spatial scale at $\xi_j = 0$ has been chosen arbitrarily in the pulse solution (15)–(18). Indeed, with any shifted copy of theses solutions a consistent quasi-stationary solution can be composed in the same way. In particular, a slow motion of this small-scale pulse position is possible. We want to determine now this slow motion. To this end, we first assume that the set of solutions to the system (31)–(34) is a N-dimensional manifold which can be locally parameterized by the pulse positions $r_1 \ldots r_N$. Hence, the further parameters can be considered as given functions

$$\begin{array}{ll} a_j(r_1 \ldots r_N), & b_j(r_1 \ldots r_N), \quad 1 \le i \le N \\ c_j(r_1 \ldots r_N), & d_j(r_1 \ldots r_N), \quad 0 \le j \le N. \end{array} \tag{40}$$

Then, we introduce the explicit time dependence $r_1(t) \ldots r_N(t)$ and assume that the other parameters a_j, b_j, c_j, d_j, follow adiabatically as

$$a_j(t) = a_j(r_1(t) \ldots r_N(t))$$

etc. For a fixed choice of pulse positions $r_1 \ldots r_N$, the quasi-stationary profile in the vicinity of the pulse at r_j is given by

$$u_j(\xi_j) = a_j + \varepsilon \int_0^{\xi_j} p_j(\eta; a_j, b_j) d\eta \tag{41}$$

$$v_j(\xi_j) \equiv v_j(\xi_j; a_j, b_j) \tag{42}$$

with

$$\xi_j = \frac{x - r_j(t)}{\varepsilon}. \tag{43}$$

Since we want to go back to the time dependent system (2), we have eliminated p as an extra independent variable by incorporating it as a first order correction for u. Inserting (41) and (42) into the v-equation of (2) and taking into account the explicit time dependence of the pulse parameters, we obtain

$$\frac{\partial v_j}{\partial \xi_j}\dot{\xi}_j + \frac{\partial v_j}{\partial a_j}\sum_{k=1}^{N}\frac{\partial a_j}{\partial r_k}\dot{r}_k = \varepsilon g'(a_j)v_j^2\int_0^{\xi_j} p(\eta; a_j, b_j)d\eta + O(\varepsilon^2). \tag{44}$$

On the right hand side we have used Taylor expansion and (9), (10) to cancel leading order terms. Now we multiply with the derivative of the pulse $\frac{\partial v_j}{\partial \xi_j}$ and integrate. In this way we can isolate the small-scale pulse velocity $\dot{\xi}_j$. This procedure can be understood as a leading order approximation of the projection to the generator of the shift of the pulse. Note that according to (41) the u component of the pulse is in leading order constant. This justifies, that we neglect here the u-equation of (2), being multiplied with a derivative of order ε. Note that even though the system is not self adjoint, the shift mode coincides with its adjoint in leading order. Taking into account that

$$\int_{-\infty}^{\infty}\frac{\partial v_j}{\partial \xi_j}\frac{\partial v_j}{\partial a_j}d\xi_j = 0,$$

we obtain from this procedure

$$\dot{\xi}_j\int_{-\infty}^{\infty}\left(\frac{\partial v_j}{\partial \xi_j}\right)^2 d\xi_j = \varepsilon g'(a_j)\int_{-\infty}^{\infty}\frac{\partial v_j}{\partial \xi_j}v_j^2\int_0^{\xi_j} p(\eta; a_j, b_j)d\eta d\xi_j. \tag{45}$$

Using partial integration, recalling the expressions for v_j^3 and $\left(\frac{\partial v_j}{\partial \xi_j}\right)^2$ from (17) and (18), and employing known integrals for them we derive

$$\dot{\xi}_j = -\frac{\varepsilon g'(a_j)\int_{-\infty}^{\infty}\frac{v_j^3}{3}(p(\xi_j; a_j, b_j))d\xi_j}{\int_{-\infty}^{\infty}\left(\frac{\partial v_j}{\partial \xi_j}\right)^2 d\xi_j} \tag{46}$$

$$= -\frac{2\varepsilon b_j g'(a_j)}{g(a_j)}. \tag{47}$$

Taking into account equation (43), we arrive finally at

$$\dot{r}_j(t) = 2\varepsilon^2\frac{b_j(t)g'(a_j(t))}{g(a_j(t)),} \tag{48}$$

which, together with the solution of the consistency conditions (40), provides the law of motion for the pulse positions r_j, $i = 1, \ldots, N$. Since the slow motion takes place in the fine spatial scale ξ_j, it is of order ε^2 in the large scale variable r_j, which enters

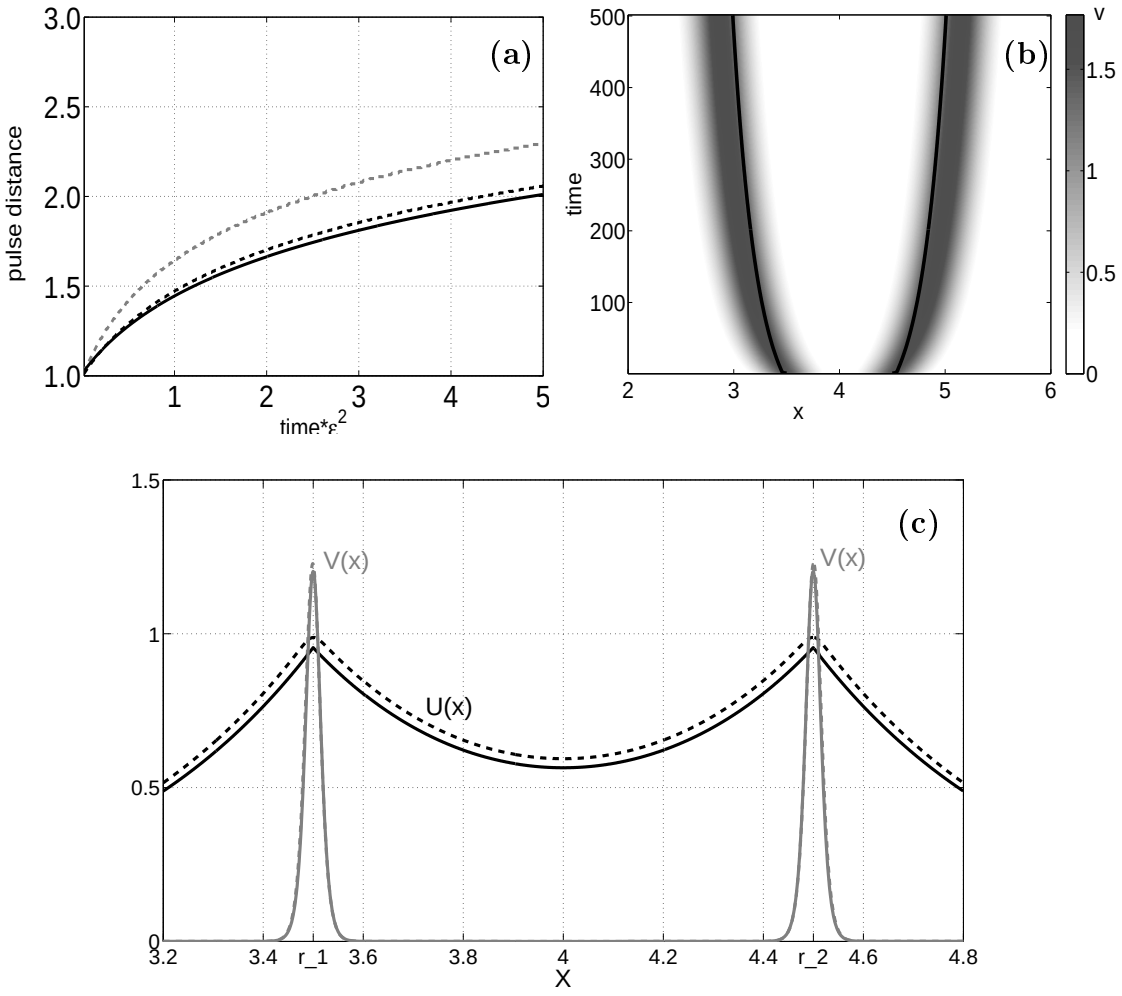

Figure 1: Pulse motion for 2-pulse solution of the modified Gierer-Meinhardt model (49) with $\mu = 5$, $\alpha = 0.2$, $L = 8$, and Neumann boundary conditions. (a) Pulse distance for numerical solutions of the full system with $\epsilon = 0.1$ (grey dashed line) and $\epsilon = 0.02$ (black dashed line) compared to the law of motion (48) (solid line). (b) v-component of the full numerical solution for $\epsilon = 0.1$ (grey-scale plot) and pulse positions (curves) predicted by (48). (c) profiles at a fixed time t: Dashed line: numerical solution of the full system; solid line: ansatz-solution (15)–(18) and (21)–(24).

into the consistency equations. Note that the motion of each pulse is determined by its local pulse parameters a_j, b_j only. However, there is a pulse interaction, since these parameters depend via (40) on the other pulse positions.

In Figure 1 we compare the effective pulse motion given by (48) with a numerical solution for the full system, calculating the motion of a pair of two symmetric interacting pulses of the modified Gierer-Meinhardt model (details of this model

will be given in the next section). Panel (a) shows the pulse distance as a function of time. As soon as the pulses are well separated, the effective pulse motion according to (48) (solid curve) is in good coincidence with the distance of the maxima of a numerical solution for the full system. Already for moderately small $\varepsilon = 0.1$ (grey dashed line) the agreement is reasonably good and improves significantly for the smaller value $\varepsilon = 0.02$ (black dashed line).

4 Interacting pulse solutions of the Gierer-Meinhardt system

We apply now the general results from the preceeding sections to study manifolds of interacting pulse solutions for a specific system. As an example, we have chosen the well known Gierer-Meinhardt system [10] with a modification introduced in [3]. Specifying the nonlinearities

$$f(U) := 1, \qquad g(U) := \frac{1}{U} + \alpha \tag{49}$$

in our general system (1), we obtain for $\alpha = 0$ the classical Gierer-Meinhardt system, and for $\alpha > 0$ the modified version from [3].

4.1 1-pulse solutions

As a warm up, we begin with solutions having a single pulse that interacts with the boundary under Neumann boundary conditions. From the six consistency conditions, given by (31)-(34) with $j = 1$ and (35), the pulse parameters c_0, c_1, d_0, d_1 can be easily eliminated, and we remain with

$$a_1\sqrt{\mu}(\tanh(\sqrt{\mu}r_1) + \tanh(\sqrt{\mu}(L - r_1))) = \frac{6f(a_1)}{g^2(a_1)} \tag{50}$$

$$a_1\sqrt{\mu}(\tanh(\sqrt{\mu}r_1) - \tanh(\sqrt{\mu}(L - r_1))) = 2b_1. \tag{51}$$

Inserting the Gierer-Meinhardt nonlinearities (49) with $\alpha = 0$, equation (50) has the solution

$$6a_1 = \sqrt{\mu}(\tanh(\sqrt{\mu}r_1) + \tanh(\sqrt{\mu}(L - r_1))),$$

and the pulse motion from (48) is given by

$$\dot{r}_1 = \varepsilon^2(\tanh(\sqrt{\mu}(L - r_1)) - \tanh(\sqrt{\mu}r_1)). \tag{52}$$

This implies that on the one-dimensional manifold of quasi-stationary 1-pulse solutions there is a unique globally stable equilibrium with the pulse at $r_1 = L/2$.

For $\alpha > 0$, equation (50) reads

$$\frac{6a_1}{(1 + \alpha a_1)^2} = \sqrt{\mu}(\tanh(\sqrt{\mu}r_1) + \tanh(\sqrt{\mu}(L - r_1))).$$

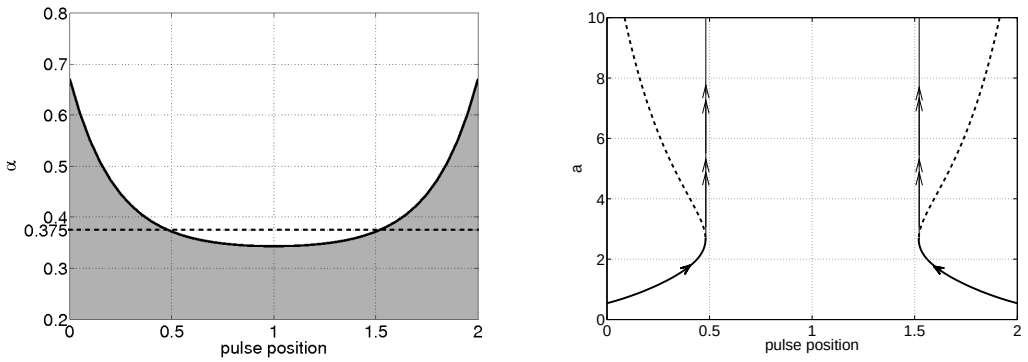

Figure 2: Left panel: Fold line and existence region (grey) for 1-pulse solutions ($L = 2$, $\mu = 5$); right panel: stable and unstable (dashed) branches for $\alpha = 0.375$. Arrows and thin lines indicate slow motion and fast drop-off at the fold

This equation is quadratic in a_1 and has two real solutions, if

$$\sqrt{\mu}\alpha(\tanh(\sqrt{\mu}r_1) + \tanh(\sqrt{\mu}(L - r_1))) \leq \frac{3}{2}. \tag{53}$$

The shaded region in Figure 2 shows the pulse positions in the domain $[0, L]$ for $L = 2$ where two branches of 1-pulse solutions coexist. When (53) holds with equality, these two branches meet in a fold, which is represented by the black line in figure 2. Above this line (white region) no 1-pulse solution exists. The height of the fold-point is given by

$$a_1 = a_F = \frac{1}{\alpha}.$$

Our numerical simulations of the full system indicate, that the the branch with $a_1 < a_F$ is stable. The pulse motion is now given by

$$\dot{r}_1 = \varepsilon^2 \frac{\alpha\mu(\tanh^2(\sqrt{\mu}(L - r_1)) - \tanh^2(\sqrt{\mu}r_1))}{3 \pm \sqrt{9 - 6\alpha\sqrt{\mu}(\tanh(\sqrt{\mu}r_1) + \tanh(\sqrt{\mu}(L - r_1)))}} \tag{54}$$

(compare (52)), showing that the stationary pulse at $r_1 = L/2$, as long as it exists, is still globally stable within the stable branch of the slow manifold. For

$$\alpha\sqrt{\mu}\tanh(\sqrt{\mu}L/2) > \frac{3}{4} \tag{55}$$

the pulse at $r_1 = L/2$ does no longer exist, but a pulse located close to the boundary still moves towards the middle of the domain until it reaches the fold. There, the solution drops off the slow manifold and diverges in a fast motion towards infinity (see in the lower panel of Figure 2).

4.2 2-pulse solutions

To keep calculations simple, we will first investigate the case of an unbounded domain. The ten consistency conditions (31)–(34) for $j = 1, 2$, and (37), (39) can be

simplified to

$$\left(a_1 - \frac{3f(a_1)}{\sqrt{\mu}g^2(a_1)}\right) e^{\sqrt{\mu}(r_2-r_1)} = \frac{3f(a_2)}{\sqrt{\mu}g^2(a_2)} \tag{56}$$

$$\left(a_2 - \frac{3f(a_2)}{\sqrt{\mu}g^2(a_2)}\right) e^{\sqrt{\mu}(r_2-r_1)} = \frac{3f(a_1)}{\sqrt{\mu}g^2(a_1)} \tag{57}$$

Note that for $a_1 = a_2$ these equations coincide both with (50) after inserting there $L = \infty$. Indeed, a symmetric 2-pulse can be seen as an 1-pulse on the positive half-axis with a Neumann boundary condition at zero. In this way, existence and motion of symmetric 2-pulses are given by corresponding expressions from the previous section. The branch of symmetric solutions can be parameterized by

$$r_2 - r_1 = -\frac{1}{\sqrt{\mu}} \ln\left(\frac{\sqrt{\mu}}{3}\left(\frac{1}{a_1} + 2\alpha + \alpha a_1\right) - 1\right).$$

For

$$\alpha\sqrt{\mu} < \frac{3}{4}$$

there are two symmetric 2-pulse solutions for each pulse distance (compare (55). This condition already has been derived in [3] (eq. 5.3). For larger values of $\alpha\sqrt{\mu}$ the two branches meet in a fold with

$$a_1 = a_F = \frac{1}{\alpha},$$

and there is a maximal pulse distance given by

$$r_2 - r_1 = y_F = -\frac{1}{\sqrt{\mu}} \ln\left(\frac{4\alpha\sqrt{\mu}}{3} - 1\right).$$

Now we look for non-symmetric 2-pulse solutions.To this end, we eliminate the pulse distance $r_2 - r_1$ from the equations (56) and (57) and obtain

$$G(a_1) = G(a_2)$$

with

$$G(a) := \left(a - \frac{3f(a)}{\sqrt{\mu}g^2(a)}\right) \frac{f(a)}{g^2(a)}.$$

For symmetric 2-pulse solutions, this equation is trivially satisfied. Non-symmetric solutions arise, if the function G is not monotone. Inserting the nonlinearities (49), differentiating, and calculating the discriminant of the resulting third order polynomial, one can find that non-monotonicity appears for the modified Gierer-Meinhardt system with

$$\alpha\sqrt{\mu} \leq \frac{33\sqrt{33} - 177}{16}. \tag{58}$$

Remarkably, the bifurcation is again governed by the product $\alpha\sqrt{\mu}$.

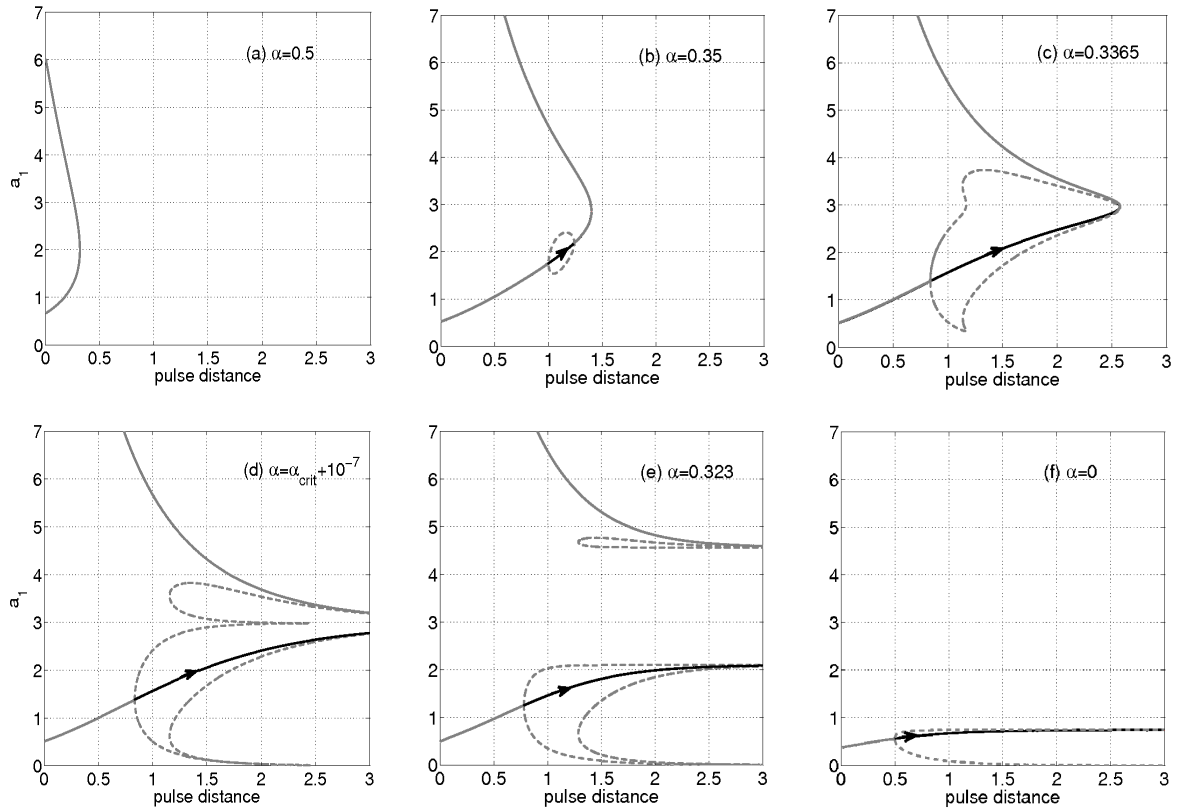

Figure 3: Manifolds of symmetric (solid lines) and asymmetric (dashed lines) 2-pulse solutions for the modified Gierer-Meinhardt system with $\mu = 5$ and different values of α (unbounded domain). Stability (bold) has been detected by numerical simulation of the full system. Arrows indicate the direction of stable slow motion, given by equation (48).

At this point we invoke a numerical solution of the consistency equations (56) and (57). Using continuation methods, we obtain the manifolds depicted in Figure 3. We have fixed $\mu = 5$ and display the manifolds of 2-pulse solutions for different values of α. For $\alpha = 0.5$ inequality (58) does not hold true and there is only the folded branch of symmetric solutions. As a 1-pulse solution on the positive half-axis with a Neumann boundary condition at zero, the lower part of this branch is stable. As a symmetric 2-pulse, however, it turns out to be unstable with respect to symmetry-breaking perturbations. For $\alpha = 0.35$ inequality (58) is satisfied and a small bubble of non-symmetric 2-pulse solutions has appeared. At the same time the symmetric branch in the interior has become stable. For further decreasing values of α, the stable part increases until for $\alpha = \frac{3}{4\sqrt{\mu}}$ the fold of the symmetric branch disappears to infinity. At the same time the asymmetric branch becomes unbounded an separates

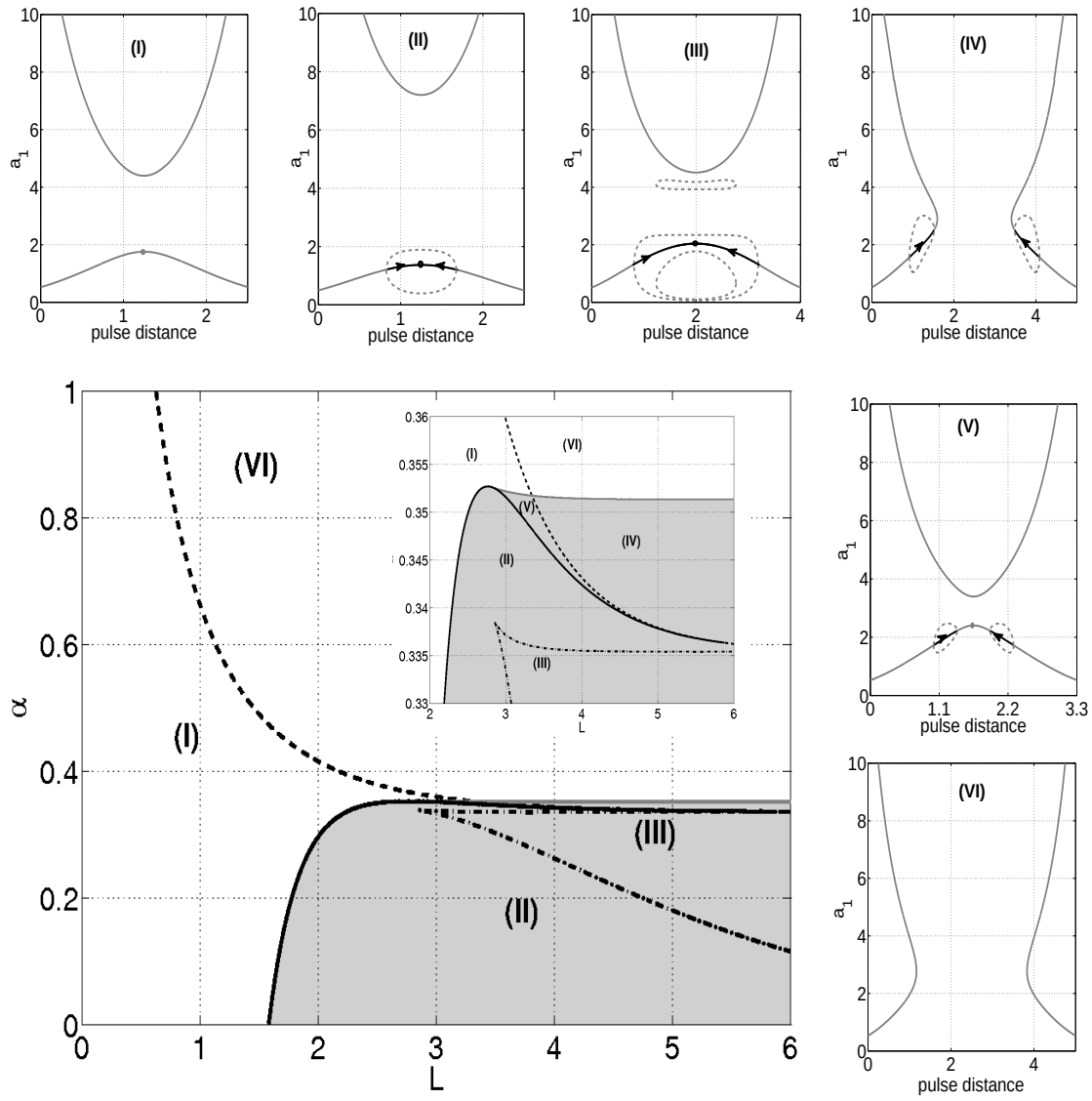

Figure 4: Panels (I)–(VI): configurations of manifolds of 2-pulse solutions for different choices of L and α (periodic boundary conditions). Large figure: Bifurcation diagram, indicating transitions between these configurations at singularities of different types. Grey area: existence of stable 2-pulse solutions

into two components. Panels (d) and (e) show the situation short before and after this transition. The arrows depict the direction of the drift of the stable two-pulse solutions given by (48).

Note that the stable parts of the manifolds loose their stability here in a symmetry-breaking pitchfork, where a branch of symmetric solutions is crossed by a branch of asymmetric solutions. The fold, which was the reason for the loss of stability of the 1-pulse, occurs here at an already unstable part of the slow manifold. Anyhow, the fold points (there appear also several on the asymmetric branch) should correspond to points of normal non-hyperbolicity, where a persistence of the slow manifold can

not be expected. The symmetry-breaking pitchfork explains also the asymmetric blow-up, which was observed numerically in [3]. Figure 3 shows that for the value $\alpha = 0.342$ used in [3] the fold and the pitchfork are so close that by numerical simulation they are hardly to distinguish. This is however only a coincidence, which does not hold true for other values of α.

Finally, we investigate the case of periodic boundary conditions. Here, the length L of the interval enters as a further parameter. Again, there are ten consistency conditions from (31)–(34) for $j = 1, 2$ and from the boundary conditions. They can be simplified to

$$a_1(\sinh(\sqrt{\mu}(L-x)) + \sinh(\sqrt{\mu}x)) - a_2 \sinh(\sqrt{\mu}L) + 2\frac{3f(a_2)}{\sqrt{\mu}g^2(a_2)} = 0 \qquad (59)$$

$$a_2(\sinh(\sqrt{\mu}(L-x)) + \sinh(\sqrt{\mu}x)) - a_1 \sinh(\sqrt{\mu}L) + 2\frac{3f(a_1)}{\sqrt{\mu}g^2(a_1)} = 0. \qquad (60)$$

By numerical continuation methods, we obtain the manifolds of symmetric and asymmetric 2-pulse solutions, depending on the chosen values of L and α. Panels (I)-(VI) show different configurations: In (I) and (VI) there are no stable 2-pulse solutions. In (II) and (III), there is a stable stationary symmetric 2-pulse to which the other stable 2-pulses converge. In (IV) and (V), the stable 2-pulses move into a pitchfork instability, as described above. The picture is completed by a bifurcation diagram in the parameters L and α, indicating singularities that lead to transitions between the configurations (I)–(VI): The solid lines are degenerate pitchforks, at which bubbles of asymmetric solutions merge or emerge at a symmetric solution. The dashed line corresponds to a branch-switching of the symmetric solutions and the dashed-dotted line to the emergence of the second asymmetric branch. Note that for $L \to \infty$ the scenarios (VI), (IV), (III), and (II) correspond precisely to the diagrams (a), (b), (e), and (f) of the figure 3 for the unbounded domain.

5 Conclusions

We present here an systematic approach to the problem of semistrong interaction, based on classical concepts of singular perturbation theory. It can be applied to a variety of problems with interacting steep fronts or pulses and a varying background between them. A similar approach has been applied to the interaction of optical pulses in mode-locked semiconductor lasers [14]. The singular perturbation approach comes in two stages. First, we are looking for quasi-stationary solutions of the original problem, which finally will constitute a slow-motion manifold. In contrast to ODEs, where the stationary problem is just an algebraic equation whose leading order solutions supply immediately a leading order approximation of the slow manifold, the stationary problem is here a singularly perturbed ODE in the spatial variable. Solutions to this equation may consist of slow and fast parts. Since the evolution takes place in the spatial variable of the original system, these correspond to small scale parts, which are in fact the fronts or pulses, and large scale

parts, which are the background between the pulses. In order to obtain a leading order approximation for the solutions, it is sufficient to solve the fast and slow subproblems separately and then compose them to a global approximating solution. Solutions to the slow and fast subproblem appear usually in families depending on a finite number of parameters, such as e.g. pulse positions or pulse heights. Gluing the piecewise slow and fast solutions together induces nonlinear constraints between these parameters. The full set set of leading order solutions is then found as the solution manifold to the system of constraints in the space of parameters of all the subproblems. For the specific structure of the systems introduced in [3] and presented here the subproblems can be solved analytically and hence the constraints can be written as simple algebraic expressions, allowing for a detailed qualitative investigation of the resulting manifolds. Using numerical path-following techniques already at an earlier stage, it would also be possible to treat more complicated problems in a similar manner.

In a second step, we have used higher order terms to determine the slow motion along the manifolds of quasi-stationary solutions. This is based on the assumption that the manifolds are normally hyperbolic and hence persist for $\varepsilon > 0$. This assumption should of course be verified in a rigorous way. Our investigations show that normal hyperbolicity breaks down as soon as the manifold is not parametrized by the pulse positions. In this way we were able not only to describe the semistrong interaction, but also the breakdown of this regime in two different scenarios.

In the derivation of the equation (48) for the slow motion of the interacting pulses, we discover the strange fact that the motion does not take place in the next order, but is only of order ε^2. This is related to the fact that the small scale pulse problem (5), (6) is reversible and hence has a generic homoclinic solution. At that point one could introduce pulse velocities of order one in the small spatial scale as additional solution parameters, which in general have not to be identically zero as in this particular case.

References

[1] A. Afendikov, A.Mielke,*Multi-pulse solutions to the Navier-Stokes problem between parallel plates*, Z. Angew. Math. Phys. **52** (2001) no. 1 79-100

[2] J.Carr and R.Pego, *Metastable patterns in solutions of* $u_t = e^2 u_{xx} - f(u)$, Comm. Pure Appl. Math **42** (1989), 523-576 .

[3] A. Doelman, T. Kaper, *Semistrong Pulse Interaction in a Class of Coupled Reaction-Diffusion Equations*, SIAM J. Applied Dynamical Systems **2** (2003), no. 1, 53-96

[4] A.Doelman, W. Eckhaus, T.J. Kaper, *Slowly modulated two-pulse solutions in the Gray-Scott model I: Asymptotic construction and stability* SIAM J. Appl. Math. **61** (2000), 1080-1102

[5] A.Doelman, W. Eckhaus, T.J. Kaper, *Slowly modulated two-pulse solutions in the Gray-Scott model II: Geometric theory, bifurcations, and splitting dynamics* SIAM J. Appl. Math. **61** (2001), 2036-2062

[6] A. Doelman, T.J. Kaper, H. van der Ploeg, *Spatially periodic multi-pulse patterns in the one-dimensional Gierer-Meinhardt equations*, Indiana Univ. Math. J. **50** (2001), 443-507

[7] A. Doelman, R. A. Gardner, T.J. Kaper, *Large stable pulse solutions in reaction-diffusion equations*, Methods Appl. Anal. **8** (2001), 387-414

[8] A. Doelman, T.J. Kaper, P. Zegeling, *Pattern formation in the one-dimensional Gray-Scott model*, Nonlinearity **10** (1997), 523-563

[9] S. Ei, *The motion of Weakly Interacting Pulses in Reaction-Diffusion Systems*, J. of Dynamics and Diff. Equations **14** (2002) no. 1, 85-137

[10] A.Gierer, H. Meinhardt, *A Theory of Biological Pattern Formation*, Kybernetik **12** (1972), 30-39

[11] P.Gray, S.K. Scott, *Autocatalytic reactions in the isothermal, continous stirred tank reactor: isolas and other forms of multistability*, Chem. Eng. Sci. **38** (1983), 29-43

[12] P.Gray, S.K. Scott, *Autocatalytic reactions in the isothermal, continous stirred tank reactor: Oscillations and instabilities in the system* $A+2B \to 3B, C \to C$, Chem. Eng. Sci. **39** (1984), 1087-1097

[13] J. D. Murray, *Mathematical Biology*, Interdisciplinary Mathematics Series, Vol. 17, 3rd. ed. (2002)

[14] M. Nizette, D. Rachinskii, A. Vladimirov, M. Wolfrum, *Pulse interaction via gain and loss dynamics in passive mode-locking*, Physica D **218**(1) (2006), 95-104

[15] B. Sandstede, *Stability of travelling waves*, in Handbook of Dynamical Systems, Vol. 2 (Ed.: B. Fiedler), Elsevier (2002)

[16] M.J. Ward, J. Wei, *Asymmetric spike patterns for the one-dimensional Gierer-Meinhardt model:equilibria and stability*, European J. Applied Math **13** (2003), no. 3, 283-320

[17] H. Weinberger, *On metastable patterns in parabolic systems*, Rend. Accad. Naz. Lincei **77** (1986), 291-313

[18] S. Zelik, A. Mielke, *Multi-pulse evolution and space-time chaos in dissipative systems* WIAS Preprint (2006)